THE UNIVERSITY of EDINBURGH

Edinburgh Research Explorer

Effect of micropillar spacing and temperature of substrate on contact angle dynamics

Citation for published version:
Dover, C, Duursma, G, Sefiane, K, Christy, J & Terry, J 2018, 'Effect of micropillar spacing and temperature of substrate on contact angle dynamics', *Heat Transfer Engineering*.
https://doi.org/10.1080/01457632.2018.1443246

Digital Object Identifier (DOI):
10.1080/01457632.2018.1443246

Link:
Link to publication record in Edinburgh Research Explorer

Document Version:
Peer reviewed version

Published In:
Heat Transfer Engineering

General rights
Copyright for the publications made accessible via the Edinburgh Research Explorer is retained by the author(s) and / or other copyright owners and it is a condition of accessing these publications that users recognise and abide by the legal requirements associated with these rights.

Take down policy
The University of Edinburgh has made every reasonable effort to ensure that Edinburgh Research Explorer content complies with UK legislation. If you believe that the public display of this file breaches copyright please contact openaccess@ed.ac.uk providing details, and we will remove access to the work immediately and investigate your claim.

Download date: 06. May. 2023

Effect of micropillar spacing and temperature of substrate on contact angle dynamics

Coinneach Mackenzie-Dover[1], Gail Duursma[1*], John Christy[1], Jonathan G. Terry[1], Khellil Sefiane[1,2]

[1]School of Engineering, The University of Edinburgh, King's Buildings, Mayfield Road, Edinburgh EH9 3JL, United Kingdom

[2]Tianjin Key Lab of Refrigeration Technology, Tianjin University of Commerce, Tianjin City 300134, PR China

[*]Address correspondence to Dr Gail Duursma, School of Engineering, The University of Edinburgh, The King's Buildings, Mayfield Road, Edinburgh EH9 3JL, UK
E-mail: gail.duursma@ed.ac.uk
Phone Number: 0 (+44) 131 650 4868, Fax Number: 0 (+44) 131 650 6551

ABSTRACT

Contact angle dynamics of droplets deposited on a structured surface were studied in this work and the effects of substrate microstructure and temperature were investigated. Microstructures consisting of uniformly-sized, cubic micropillars with varying pillar spacings were constructed by microfabrication. Droplets (of the order of tens of microlitres in volume) were deposited on these surfaces and dynamic contact angles were observed using various techniques. Advancing and receding contact angles were measured using tilting of the surfaces or by injection and aspiration of fluid from a horizontal droplet by syringe. Droplets on these surfaces appeared to be mainly in the Wenzel state. Contact angle hysteresis was obtained as a function of pillar spacing or, equivalently, surface roughness. Depinning force was deduced and a linear dependence on maximal three phase contact line was found. The techniques of tilting the surface on which the droplet was deposited and uniformly increasing and reducing the volume of the droplet via the syringe both gave the same contact angle hysteresis for a given micropillar spacing. The effect of temperature was then assessed using a heated tilting plate. Contact angle hysteresis was found to increase with temperature. Further work to elucidate mechanisms governing this dependence will be undertaken.

.

INTRODUCTION

The dynamics of the contact angles of droplets are important to a number of industrial and biological applications whether motion be induced by gravity, forced by injection or resulting from droplet evaporation [1-5]. In motion induced by tilting and by injection into droplets, both advancing and receding contact angles occur whereas only receding contact angles are observed in droplet evaporation [5,6]. The microstructure of the surface on which the droplet sits is fundamental to the dynamics of the contact angle. A direct relationship between contact angle dynamics and surface microstructure is lacking and essential for the tailoring of surfaces for industrial applications. In this work, we explore the dynamics of contact angles on manufactured microstructured surfaces comprising regular arrays of micropillars, with experiments conducted both at ambient temperature and for a heated substrate.

McHale *et al.* [1] undertook a theoretical study of contact angles on superhydrophobic surfaces, for Wenzel and Cassie-Baxter surfaces which represent two ways in which the surface structure affects contact angle. The Wenzel state represents the total wetting scenario and Cassie-Baxter represents the scenario of air pockets trapped underneath the droplet in the microstructure: since the intrinsic surface tension of the droplet is sufficient to suspend the droplet between structures; water interfaces with the surface of the pillars and interfaces with air in between pillars. The Wenzel state is represented by equation (1) and Cassie-Baxter by equation (2). They obtained expressions for the Wenzel and Cassie-Baxter contact angles relative to the contact angle on a smooth surface, respectively:

$$\cos\theta' = f\cos\theta \qquad (1)$$

$$\cos\theta' = \Phi_S\cos\theta + \Phi_S - 1 \qquad (2)$$

where θ is the contact angle on a flat surface and θ' is the contact angle on the same surface with asperity. The effect of the coarseness of the surface is quantified by the roughness factor, f. This is the ratio of the actual surface area to the geometrically projected surface area and structuring of an intrinsically hydrophobic surface enhances the hydrophobicity. Φ_S is the proportion of the solid surface that is in contact with liquid. McHale *et al*. [1] then derived contact angle operating points and were able to demonstrate contact angle hysteresis.

Droplets are initially pinned on these rough surfaces. Depinning occurs when droplets undergo injection (feeding or aspiration); depinning also occurs when the substrate is tilted and droplet motion is induced. Droplet depinning also occurs during evaporation and concepts from such studies may be applied to injection and titling systems though there is no analogue to an advancing contact angle in evaporation [5, 6].

Xu and Choi [2] studied droplet depinning during evaporation. They observed that depinning of the contact line occurred for their surfaces of circular posts, 5 μm in diameter, subject to maximisation of the contact line by wrapping around the entire perimeter of the microstructures. The maximal three-phase contact line, δ, normalised to the droplet boundary, is evaluated by:

$$\delta = \frac{\sum_{i=1}^{n} l_i}{L} \qquad (3)$$

where l_i represents the perimeter of the surface of an individual pillar and n is the number of microstructures along the three-phase contact line. L, is the apparent droplet boundary at the pillared surface. For a topographically uniform micropillared surface where the maximal three-phase contact line is close to the perimeter of the top surface of the pillars, equation (3) reduces to;

$$\delta = \frac{P}{\lambda} \tag{4}$$

where, P is the perimeter of the top surface of an individual micropillar and λ is the distance between two pillars. Xu and Choi [2] found a linear relationship between the depinning force and the maximal three-phase contact line for their circular microarrays. Additionally, they plotted the results of Öner and McCarthy [3], who measured the depinning force of droplets on square micropillared arrays, as a function of δ, and againfound a linear relationship.

Li and Amirfazli [4] used a thermodynamic approach to contact angle hysteresis for a two-dimensional structured surface and obtained a free energy barrier between thermodynamic states.

Shanahan and Sefiane [5] examined the excess surface energy and the requirement for depinning as a potential energy barrier per unit length of triple line which is overcome on depinning.

Orejon *et al.* [6] also investigated droplet depinning on hydrophilic and hydrophobic surfaces and used the Young's unbalanced force prior to movement of the contact line to determine the force required for depinning and slip of the contact line on the substrate.

In this study we examine the effect of the relative spacing of uniform arrays of square micropillars on the droplet contact angle dynamics as well as the depinning force as a function of the maximal three phase contact line. Moreover, most studies in literature dealing with hysteresis on structured surfaces do not study the effect of substrate heating. The effect of temperature is assessed in this study by using a heated substrate and tilting experiments.

Depinning initiates dynamic motion of the contact line and the force required to depin may be approximated from the unbalanced force at the moment of depinning:

$$F_{depinning} \cong \sigma\left|\left(\cos\theta_e - \cos\theta_{ar}\right)\right| \qquad (5)$$

In other words, the depinning force is proportional to the difference between the cosines of the equilibrium and the advancing or receding contact line when depinning occurs and the surface tension is the constant of proportionality.

The spreading and motion of the contact line after depinning has been described by either hydrodynamic theory (Cox [7], Voinov [8] and Dussan [9]) or molecular-kinetic theory (Blake and Haynes [10]). In the hydrodynamic model viscous dissipation governs the spreading process with friction in the bulk controlling contact line motion. The Cox-Voinov equation expresses the speed of contact line motion:

$$U = \frac{\sigma}{9\eta \ln\left(L/a\right)}\left(\theta^3 - \theta_e^3\right) \qquad (6)$$

where θ is the dynamic contact angle, θ_e is the equilibrium contact angle, η is the dynamic viscosity and σ the liquid-vapour surface tension. L/a is the ratio of macroscopic to microscopic length scales. Borchart-Wyart and De Gennes [11], calculating the energy dissipation per unit line length for an irreversible spreading process, obtained contact line velocity as:

$$U = \frac{\theta\sigma}{6\eta \ln\left(L/a\right)}\left(\cos\theta_e - \cos\theta\ \right) \qquad (7)$$

A result akin to this is obtained from molecular kinetic theory [10] in which spreading is considered as controlled by adsorption-desorption processes very near the contact line:

$$U = \frac{k^0 h\Lambda^3\sigma}{\eta v_m k_B T}\left(\cos\theta_e - \cos\theta\ \right) \qquad (8)$$

where k^0 is a molecular characteristic frequency, h is Planck constant, Λ is the distance between adsorption sites, v_m is the molecular flow volume, k_B is the Boltzmann constant and

T the absolute temperature. The spreading velocity is hence proportional to the ratio of driving force ($F \cong \sigma(\cos\theta_e - \cos\theta)$) and viscosity. Temperature-dependence of surface tension and viscosity leads to driving force and spreading velocity being temperature dependent as well. In this work we will assess the effect of temperature on force required to set the contact line in motion.

EXPERIMENTAL APPARATUS and PROCEDURES

Experimental surfaces were manufactured on silicon wafers at the Scottish Microelectronics Centre using photolithography and deep reactive ion etching before the surfaces were coated with Perfluorodecyltrichlorosilane (FDTS) via molecular vapour deposition. The surfaces comprised uniformly spaced arrays of 10 × 10 μm^2 square pillars and the interstructural spacing applied to distinct arrays was between 10 – 100 μm^2. A scanning electron microscope (SEM) image of a 10 ×10 μm^2 square microarray with 10 μm spacing is presented in Figure 1. This size was chosen as it can be reliably manufactured, has a significant effect on wettability and complements work of other authors [2,3].

Experimental work was carried out under atmospheric conditions. An inbuilt computer-controlled pump was used to deposit droplets of approximately 25 μl on to the experimental micro-pillared surfaces. Such droplet sizes are sufficient for the effect of structure to be present and for reliable measurement. The experimental surfaces were held in a DSA100 goniometer, which was used to measure changes to the contact angle and the contact line radius with time.

On each surface, the advancing and receding angles of the droplets were first examined using an injection technique by holding a syringe inside the droplet during feeding and aspiration, respectively, as shown in Figure 1. Water was fed into the droplet at a rate of 0.04 μl/ min

with the syringe tip held at 3 mm above the substrate surface and then withdrawn from the droplet at a rate of 0.02 μl/min with the syringe tip 1 mm from the substrate surface. These rates were chosen to obviate inertial effects.

Tilting of the substrate also revealed the advancing and receding contact angles with rate of tilt chosen to allow reliable visualisation and measurement. The substrate was tilted at a rate of 1 degree per second for room temperature experiments and 3 degrees per second for high temperature experiments; the latter to reduce the effect of evaporation. The droplets used for the high temperature study are 35 microlitres to obviate evaporative effects during the data collection. In Figure 2, images of the contact angle progression for a 25 microlitre drop is seen during a tilting experiment.

RESULTS, ANALYSIS and DISCUSSION

In Figure 3, a graph of the initial contact angle, plotted as the pillar spacing is changed, is presented. The data are fitted to the Wenzel equation for all spacings apart from the smallest which appears not to fit the Wenzel trend. This is probably due to the high surface tension of water keeping the interface in a Cassie-Baxter regime at this close spacing (or perhaps an intermediate of the two). This point is identified by the green square on the graph.

In the Wenzel mode, the liquid fills completely the space between structures. The goniometer camera could not resolve the contact line of the droplet microscopically so it not possible to confirm that the interaction at the interface between the underside of the droplet and the structured surface is that described by Wenzel, optically. Likewise, the resolution is insufficient to refute the possibility that the intrinsic surface tension of the droplet is sufficient to suspend the droplet between structures; water interfaces with the surface of the pillars and interfaces with air in between the pillars; however most of the data do not fit a Cassie-Baxter type trend.

The Wenzel and Cassie equations both allow the contact angle of a liquid on a roughened surface to be calculated if the contact angle of a liquid on an equivalent flat surface is known. The experimentally obtained values of contact angle are presented with the trendline of the Wenzel equation in Figure 3. A numerical fit of the Wenzel equation fits well with the experimental observation if the contact angle on the unstructured surface is $\theta = 97 \pm 1.7°$. This is slightly different from that reported in literature (110 degrees) but could be accounted for by roughening of the surface by the Bosch processing utilised in the production of the experimental surfaces. It is most likely then that the surface is wet by the droplet in the Wenzel mode. The results are also plotted as a function of roughness, since this is a parameter frequently used for surfaces with less regular structure. Roughness is the surface area relative to the smooth surface and is defined as:

$$roughness = \frac{actual\ area}{projected\ area} \qquad (9)$$

For the pillar spacing used here, it can be expressed as the sum of the surface area of a single micropillar and the remaining lateral area halfway between it and its eight neighbouring structures, divided by the equivalent planar area.

The advancing and receding contact angles were ascertained by two techniques: injection and tilting. For injection these angles were obtained by adding and removing water at rates of 0.04 µl/min and 0.02 µl/min, respectively. The advancing angle was judged to be exhibited by the droplet just prior to movement of initially solid contact line outwards on the images recorded by the goniometer, and the receding angle preceding closely when movement was inwards. For tilting, the substrate was set at a tilt and the angles recorded. The results for both techniques are plotted as a function of pillar spacing in Figure 4.

Though pillar spacing is an important parameter and easiest to comprehend for the pillared surfaces used in this work, for less regular surfaces, the concept of surface roughness is more

universally used. In Figures 5 and 6, the advancing and receding contact angles for injection and tilting are plotted on separate graphs as a function of surface roughness. Also included in each of these figures is the contact angle hysteresis - namely the difference in advancing and receding angles.

The depinning force is the force required to unhinge the contact line of the droplet from its anchoring sites on the surface and move the droplet radius. The Young's unbalanced force is the force acting on the contact line to effect depinning and this is due to the deviation of the contact angle from equilibrium. When the contact line moves on the surface, the force essentially quantifies the depinning force. For these experiments with tilting and with aspiration techniques, it is calculated using equation (5). It will thus be a function of pillar spacing or roughness or the maximal three phase contact line, all equivalent measures of microstructure.

Depinning force *vs* maximal three-phase contact line was plotted to obtain comparison with results in literature, and the results are shown in Figure 7. These data of depinning force measurements from our own microarrays with 10×10 μm^2 square posts using both tilting and aspiration are plotted with changing δ together with literature values of Xu and Choi [2] and Öner and McCarthy [3]. A linear relationship with depinning force is observed for both arrays from our data, as for the literature values.

It is clear that, while there is a linear relationship in each case between the depinning force and the maximal three-phase contact line, each trend has a notably distinct magnitude. It is key to establishing a direct relationship, that the factors that separate these trends are understood. The hydrophobic coating used in each study is unique; the surfaces manufactured for our work were coated in FDTS, the surfaces of Öner and McCarthy [3] were organosilane coated and the surfaces of Xu and Choi [2] were Teflon coated. It is known that both the nanostructure and surface free energy associated with hydrophobic coatings

influence significantly the interaction of hydrophobic surfaces with liquid (Feng *et al.* [12]). The most parallel trends with respect to gradient are those from the 5 μm circular micropillars of Xu and Choi [2]. Further experiments are required to probe the effect of nanoroughness, pillar morphology and pillar surface area on this promising parameter for quantifying surfaces based on their microstructure to establish a more complete picture to inform bespoke microengineering.

In this work, two techniques have been used to obtain the data, and comparison between the results is important to elucidate. Therefore for both techniques, the contact angle hysteresis, that is, the difference between the advancing and receding contact angles is plotted alongside each other in Figure 8 as a function of the roughness of the arrays. The data point associated with the most closely spaced array is an outlier.

It was seen in Figure 4 that advancing and receding angles are lower in the tilting experiments than in the case of injection. Hysteresis seen using a tilting table is slightly but systematically greater than that obtained using injection; however there is some overlap in error bars. Flow induced by gravity in the droplet may differ slightly from that of forced flow by injection; however these flows are small as the droplet is mainly changing shape. The observed hysteresis increases with roughness, which is consistent with Li and Amirfazli's [4] results for noncomposite surfaces, which levelled out for higher values – a finding we at present have insufficient data at higher roughness to confirm.

The effect of the temperature of the substrate was then investigated. Since surface tension is a function of temperature, both contact angles and their hysteresis would certainly be affected.

In Figure 9, the contact angle hysteresis of both a substrate at room temperature (23 degrees Celsius) and at 80 degrees Celsius is presented. A systematic effect of temperature is observed, with hysteresis increasing with increasing temperature. Indeed there is a complex interdependence of contact angle hysteresis on temperature. Giacomello *et al.* [13] obtained an expression for contact angle hysteresis for nanodefects which is dependent on both surface tension and excess free energy:

$$\left(\cos\theta_r - \cos\theta_a\right) = \frac{\Delta\Omega}{\sigma} \qquad (10)$$

where the right hand side is the ratio of the excess free energy at the spinodal to the surface tension.

The numerator is temperature dependent, as is the surface tension in the denominator. As the surface tension is a decreasing function of temperature, this contributes to the increase observed, but it is clearly not the only factor. The mechanistic origin of this temperature effect and the relative effects of surface tension and free energy is to be explored further in future work. The present work can have an important contribution in understanding diverse phenomena such systems involving nanofluids where roughness is generated by deposited nanoparticles [14].

CONCLUSIONS

The effect on droplet contact angle dynamics of experimental technique (tilting or injection) and temperature for droplets on microstructured surfaces was investigated. It was found that the experimental technique has only an insignificantly small effect on the dynamics and that the temperature of the substrate has a significant effect on contact angle hysteresis. This

temperature effect is expected to increase with greater increases in temperature than used in this work and these experiments will be undertaken in the future using the tilting technique.

Acknowledgements

We would like to thank MEMSstar Ltd for the coatings used in this work.

NOMENCLATURE

A	area, m^2
b	pillar spacing, μm
f	roughness factor, dimensionless
F	driving force, $mN.m^{-1}$
FDTS	perflourodecyltrichlorosilane
h	Planck constant, 6.626×10^{-34} $m^2.kg.s^{-1}$
k^0	molecular characteristic frequency, s^{-1}
k_B	Boltzman constant, 1.38×10^{-23} $m^2.kg.s^{-2}.K^{-1}$
l	perimeter, m
L	droplet boundary, m
L/a	ratio of macroscopic to microscopic length scales, dimensionless
n	number of microstructures, dimensionless
P	perimeter of a micropillar, m
SEM	scanning electron microscopy
T	absolute temperature, K
U	contact line velocity, $m.\ s^{-1}$

v_m molecular flow volume, $m^3.s^{-1}$

Greek Symbols

δ maximal three phase contact line, dimensionless

η dynamic viscosity, $kg.m^{-1}s^{-1}$

θ Angle, °

θ' Angle on flat surface, °

Φ Proportion of surface in contact with liquid, dimensionless

λ distance between pillars, m

Λ distance between adsorption sites, m

σ Surface tension, $mN.m^{-1}$

ΔΩ excess free energy, J

Subscripts

a advancing

ar advancing or receding

e equilibrium

r receding

s surface

REFERENCES

[1] McHale, G., Shirtcliffe, N.J., and Newton, M.I., Contact angle hysteresis in super-hydrophobic surfaces, *Langmuir*, vol. 20, pp. 10146-10149, 2004.

[2] Xu, W. and Choi, C.-H., From sticky to slippery droplets: Dynamics of contact line depinning on superhydrophobic surfaces, *Physical Review Letters*, vol. 109:024504, pp. 1-5, 2012.

[3] Öner, D. and McCarthy, T.J., Ultrahydrophobic surfaces: Effects of topography length scales on wettabilit*y*. *Langmuir*, vol. 16, pp. 7777-7782, 2000.

[4] Li, W., Amirfazli, A., A thermodynamic approach for determining the contact angle hysteresis for superhydrophobic surfaces*, Journal of Colloid and Interface Science*, vol. 292, pp. 195-201, 2005.

[5] Shanahan, M.E.R. and Sefiane, K., Kinetics of Triple Line Motion during Evaporation, *Proceedings of the Sixth International Symposium on Contact Angle, Wettability and Adhesion*, University of Maine, Maine USA. July 14-16, 2008.

[6] Orejon, D., Sefiane, K., Shanahan, M.E.R., Stick-slip of evaporating droplets: substrate hydrophobicity and nanoparticle concentration*, Langmuir* vol. 27, no. 21, pp. 12834-12843, 2011.

[7] Cox, R.G., The dynamics of the spreading of liquids on a solid surface. Part 1. Viscous flow, *J. Fluid Mech,.* vol. 168, pp. 169-194, 1986.

[8] Voinov, O.V., Hydrodynamics of wetting, *Fluid Dyn.* vol. 11, pp. 714-721, 1976.

[9] Dussan V, E.B., The moving contact line: the slip boundary condition, *J. Fluid Mech.,* vol. 77, pp. 665-684, 1976.

[10] Blake, T.D., and Haynes, J.M., Kinetics of liquid-liquid displacement, *J. Colloid Interface Sci.*, vol. 30, pp. 421-423, 1969.

[11] Brochard-Wyart, F., de Gennes, P.G., Dynamics of partial wetting*, Adv. Colloid Interface Sci*. vol. 39, pp. 1-11, 1992.

[12] Feng, L., Li, S., Li, Y., Li, H., Zhang, L., Zhai, J., Song, Y., Liu, B., Jiang, L., and Zhu, D., Super-Hydrophobic Surfaces: from Natural to Artificial, *Avd. Mater.*, vol. 14, no. 24, pp. 1857-1860, 2002.

[13] Giacomello, A., Schimmele, L., and Dietrich, S., Wetting hysteresis induced by nanodefects, *Proceedings of the National Academy of Sciences of the United States of America*, vol. 113, no. 3, pp. E262-E271, 2015.

[14] Duursma, Gail; Sefiane, Khellil; Kennedy, Aiden, Experimental Studies of Nanofluid Droplets in Spray Cooling, *Heat Transfer Engineering,* Vol. 30 no. 13, pp. 1108-1120, 2009.

List of Figure captions.

Figure 1: SEM image of 10 ×10 μm^2 micropillars, spaced by 10 μm (top) and images of (a) resting droplet (for initial contact angle, (b) injected droplets and (c) droplets on a tilting plate. Pillar height is 10 μm.

Figure 2: Evolution of the dynamic contact angles during a tilting experiment for 80 micron spaced pillars (a) at rest initially, (b) pinned droplet poised to move and (c) dynamic motion of the droplet.

Figure 3: Graph describing the change of initial contact angle of a 25 μl water droplet on a micropillared surface as uniformly sized pillars are moved apart; 10 μm pillars coated in FDTS and spaced 10-100 μm apart. Theoretical prediction using Wenzel's equation (continuous curve) are superimposed to show that the surface wetting is likely in the Wenzel mode. Inset graph is of these data plotted versus equivalent surface roughness and fitted to the Wenzel model. First data point (surrounded by a square) is omitted from Wenzel fit.

Figure 4: Graph of advancing and receding angles vs spacing for injection and tilt experiments. 10 μm pillar arrays increasingly spaced in increments of 10 microns from 10-100 microns. The pillars are etched in Si and coated in FDTS. The advancing angle and receding angles are ascertained by examining the behaviour of the droplet as water is added at a rate of 0.04 μl/ min by the syringe and as the droplet is aspirated by the syringe at a rate of 0.02 μl/ min, respectively. Best fits to the data are also present. The result from the smallest spacing are not included in the fit.

Figure 5: Graph of advancing and receding angles vs roughness and (inset) contact angle hysteresis for injection experiments.

Figure 6: Graph of advancing and receding angles vs roughness and (inset) contact angle hysteresis for tilting experiments.

Figure 7: Depinning force as a function of the maximal three-phase contact line. A linear trend is observed for 10 × 10 μm^2 square micropillars when depinning force is ascertained from aspirating the droplet (circles) and when determined from the receding angle observed when subjecting the droplet to tilting (trianlges). A similar trend is seen in the results of Öner and McCarthy [3], where square micropillars were examined and those of Xu and Choi [2], where circular pillars with a diameter of 5 μm were studied.

Figure 8. Contact angle hysteresis plotted versus roughness for two different experimental techniques: tilting (triangles) and injection (circles).

Figure 9: Contact angle hysteresis as a function of temperature for experiments performed at room temperature (23 degrees Celsius) and at 80 degrees Celsius.

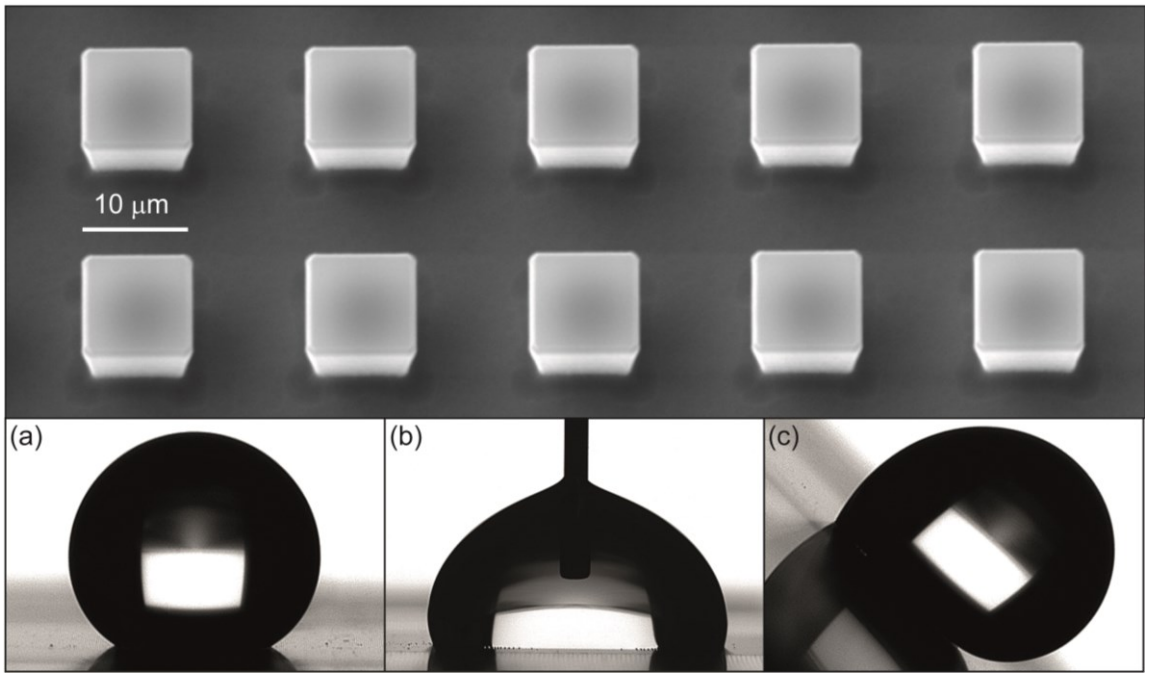

Figure 1: SEM image of 10 ×10 μm^2 micropillars, spaced by 10 μm (top) and images of (a) resting droplet (for initial contact angle, (b) injected droplets and (c) droplets on a tilting plate.

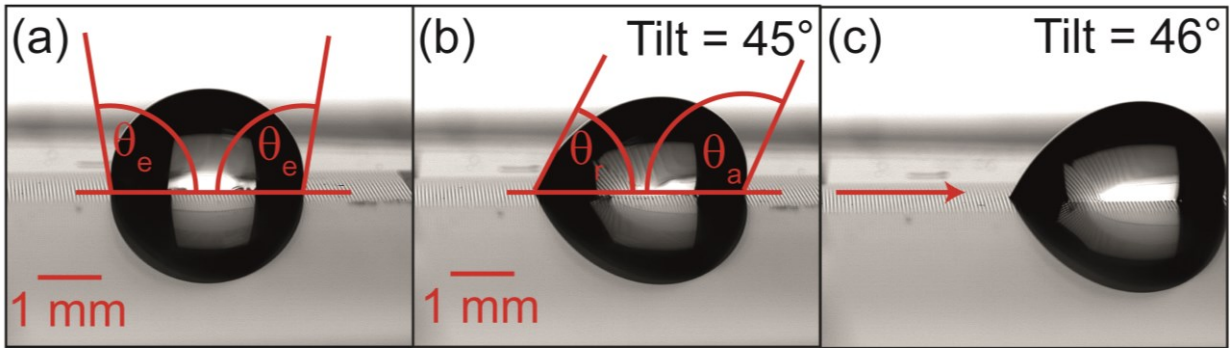

Figure 2: Evolution of the dynamic contact angles during a tilting experiment for 80 micron spaced pillars (a) at rest initially, (b) pinned droplet poised to move and (c) dynamic motion of the droplet.

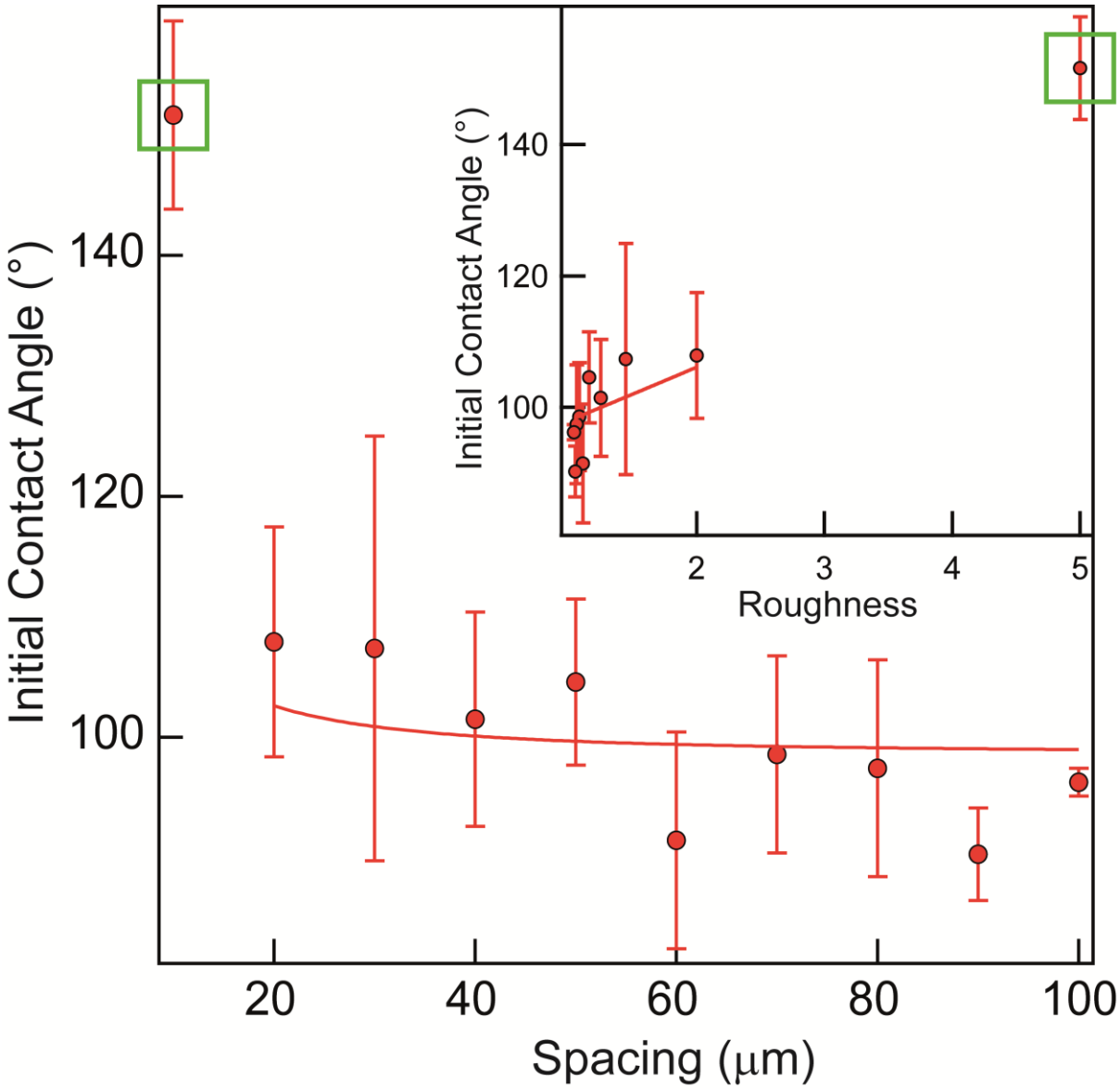

Figure 3: Graph describing the change of initial contact angle of a 25 µl water droplet on a micropillared surface as uniformly sized pillars are moved apart; 10 µm pillars coated in FDTS and spaced 10-100 µm apart. Theoretical prediction using Wenzel's equation (continuous curve) are superimposed to show that the surface wetting is likely in the Wenzel mode. Inset graph is of these data plotted versus equivalent surface roughness and fitted to the Wenzel model. First data point (surrounded by a square) is omitted from Wenzel fit.

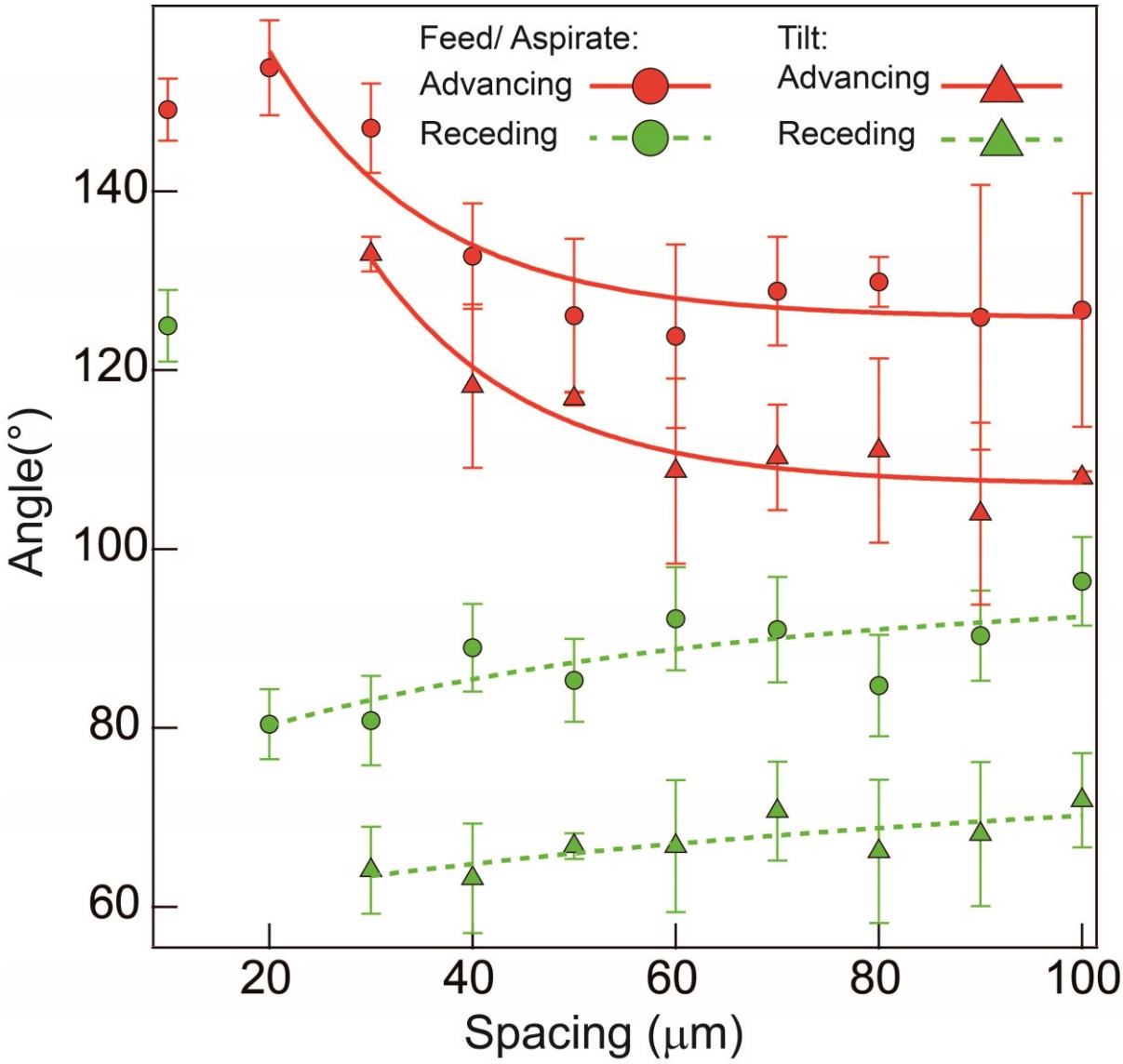

Figure 4: Graph of advancing and receding angles vs spacing for injection and tilt experiments. 10 μm pillar arrays increasingly spaced in increments of 10 microns from 10-100 microns. The pillars are etched in Si and coated in FDTS. The advancing angle and receding angles are ascertained by examining the behaviour of the droplet as water is added at a rate of 0.04 μl/ min by the syringe and as the droplet is aspirated by the syringe at a rate of 0.02 μl/ min, respectively. Best fits to the data are also present. The result from the smallest spacing are not included in the fit.

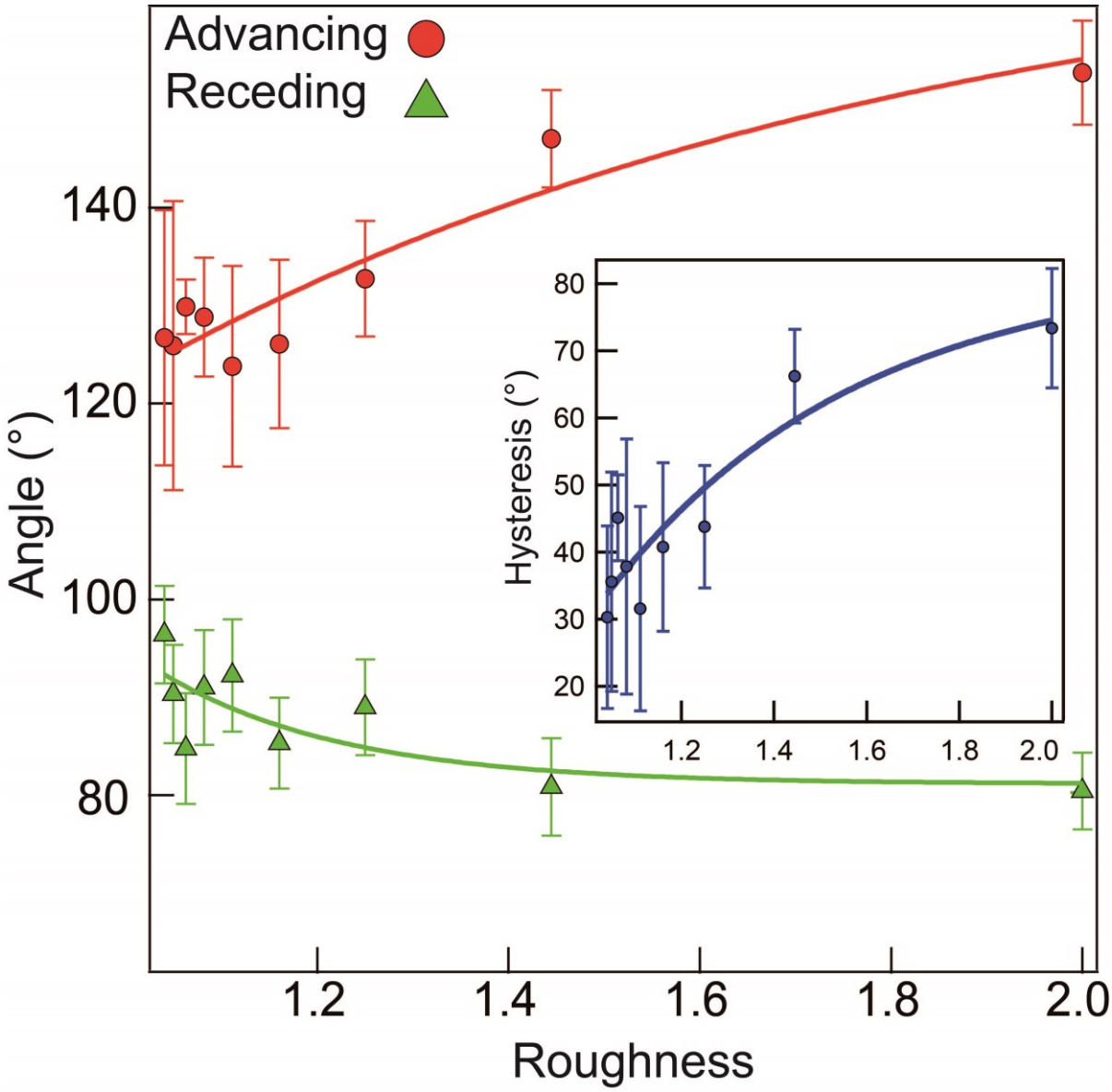

Figure 5: Graph of advancing and receding angles vs roughness and (inset) contact angle hysteresis for injection experiments.

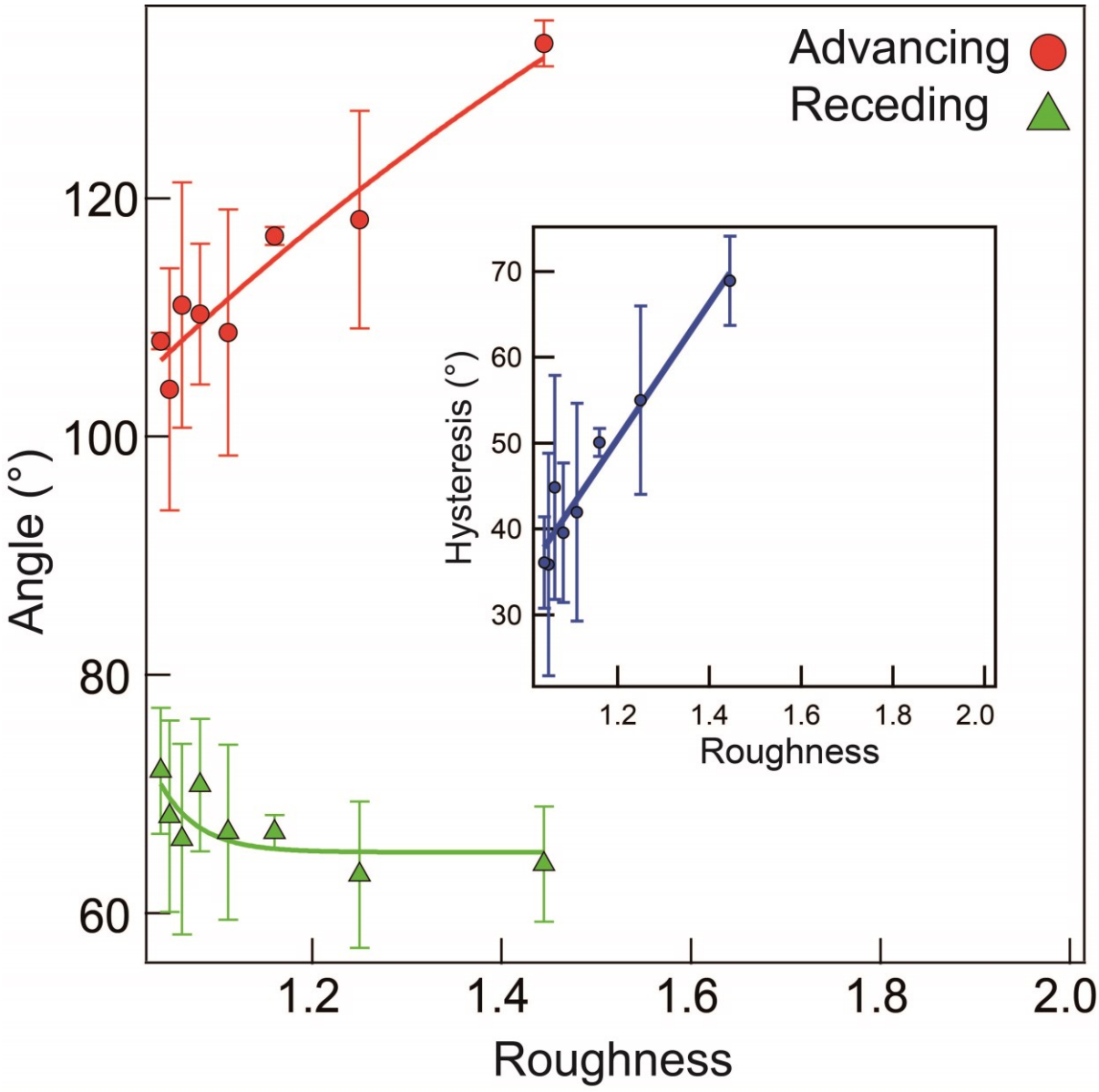

Figure 6: Graph of advancing and receding angles vs roughness and (inset) contact angle hysteresis for tilting experiments.

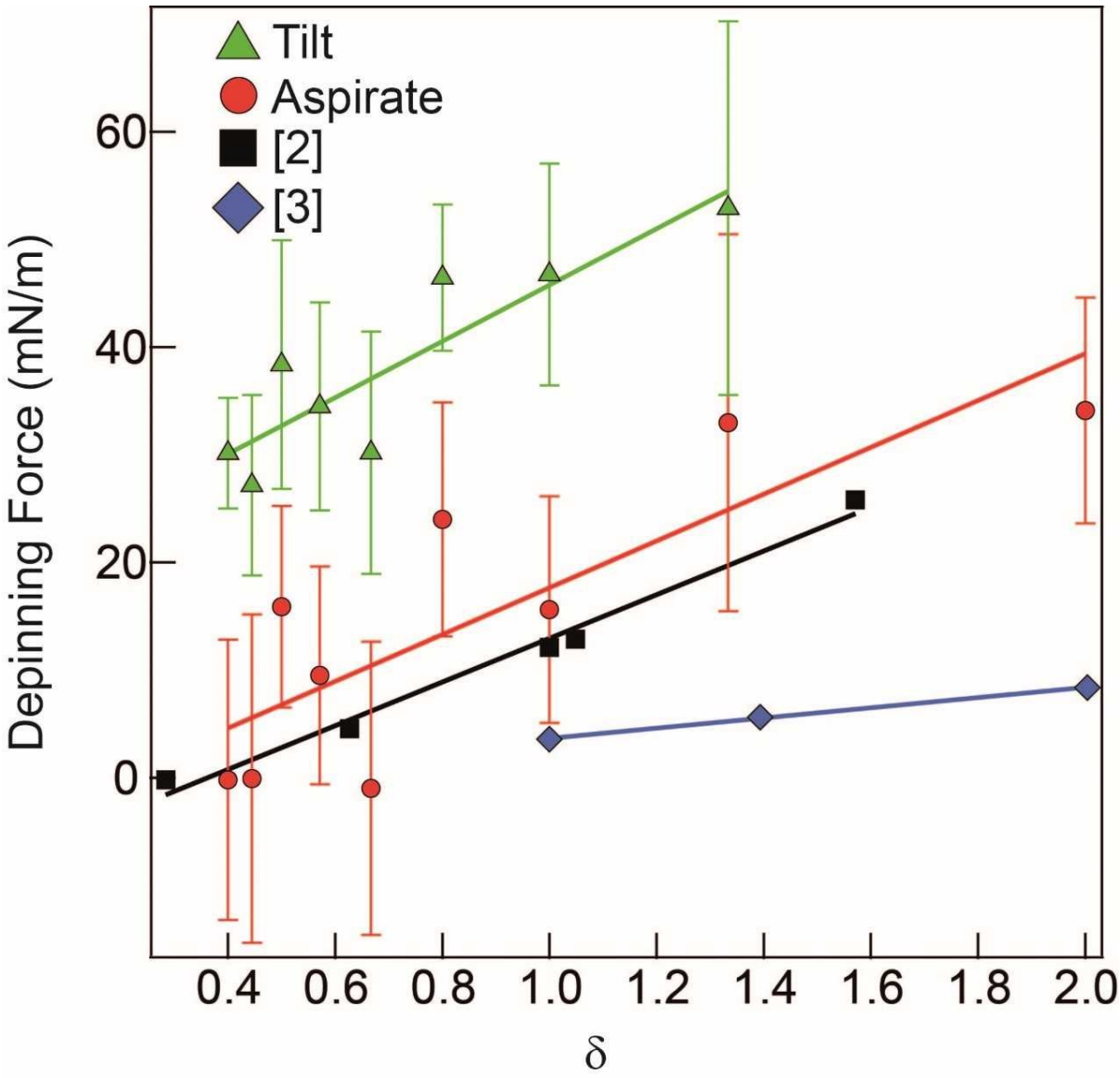

Figure 7: Depinning force as a function of the maximal three-phase contact line. A linear trend is observed for 10×10 μm^2 square micropillars when depinning force is ascertained from aspirating the droplet (circles) and when determined from the receding angle observed when subjecting the droplet to tilting (triangles). A similar trend is seen in the results of Öner and McCarthy [3], where square micropillars were examined and those of Xu and Choi [2], where circular pillars with a diameter of 5 μm were studied.

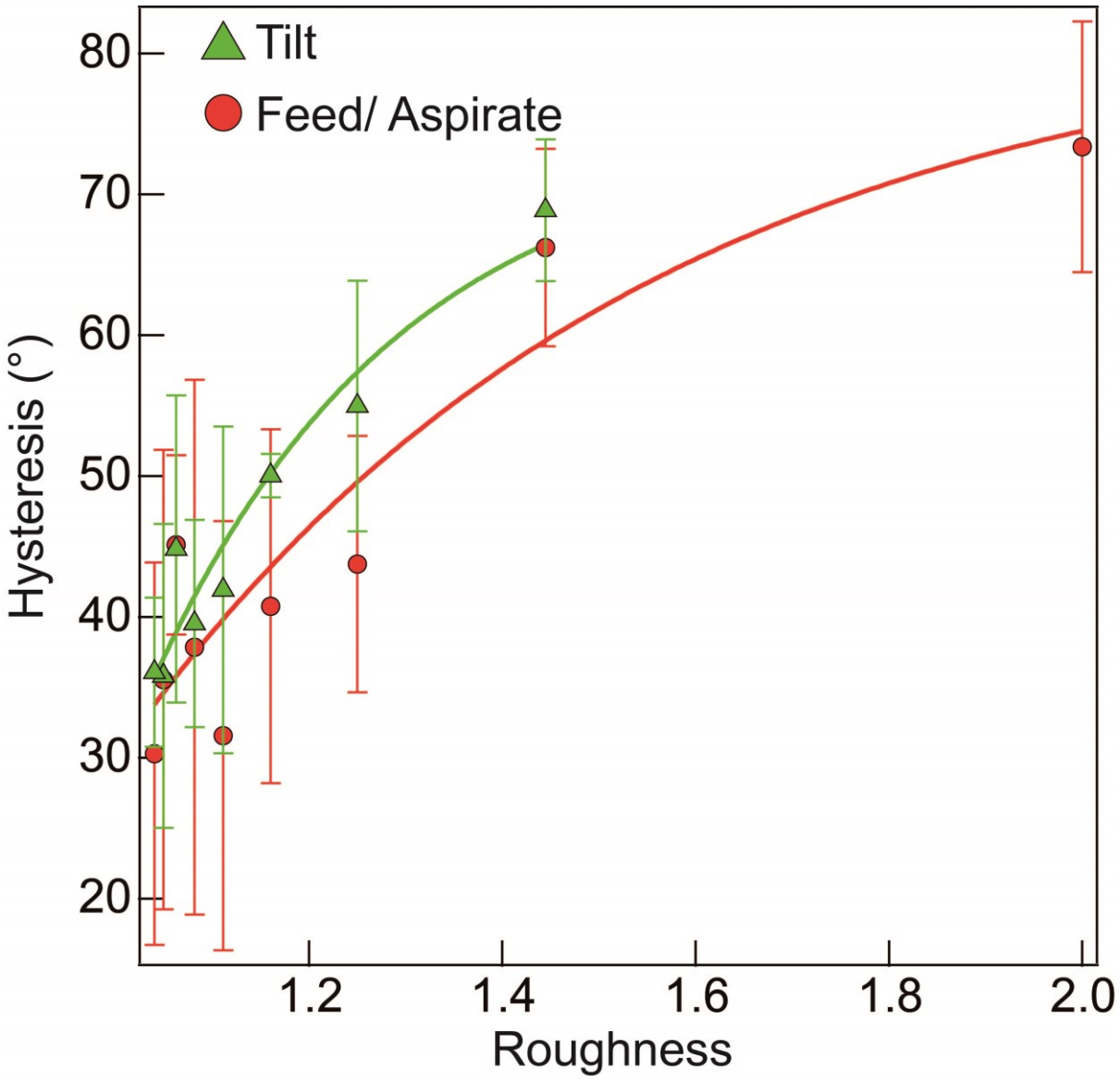

Figure 8. Contact angle hysteresis plotted versus roughness for two different experimental techniques: tilting (triangles) and injection (circles).

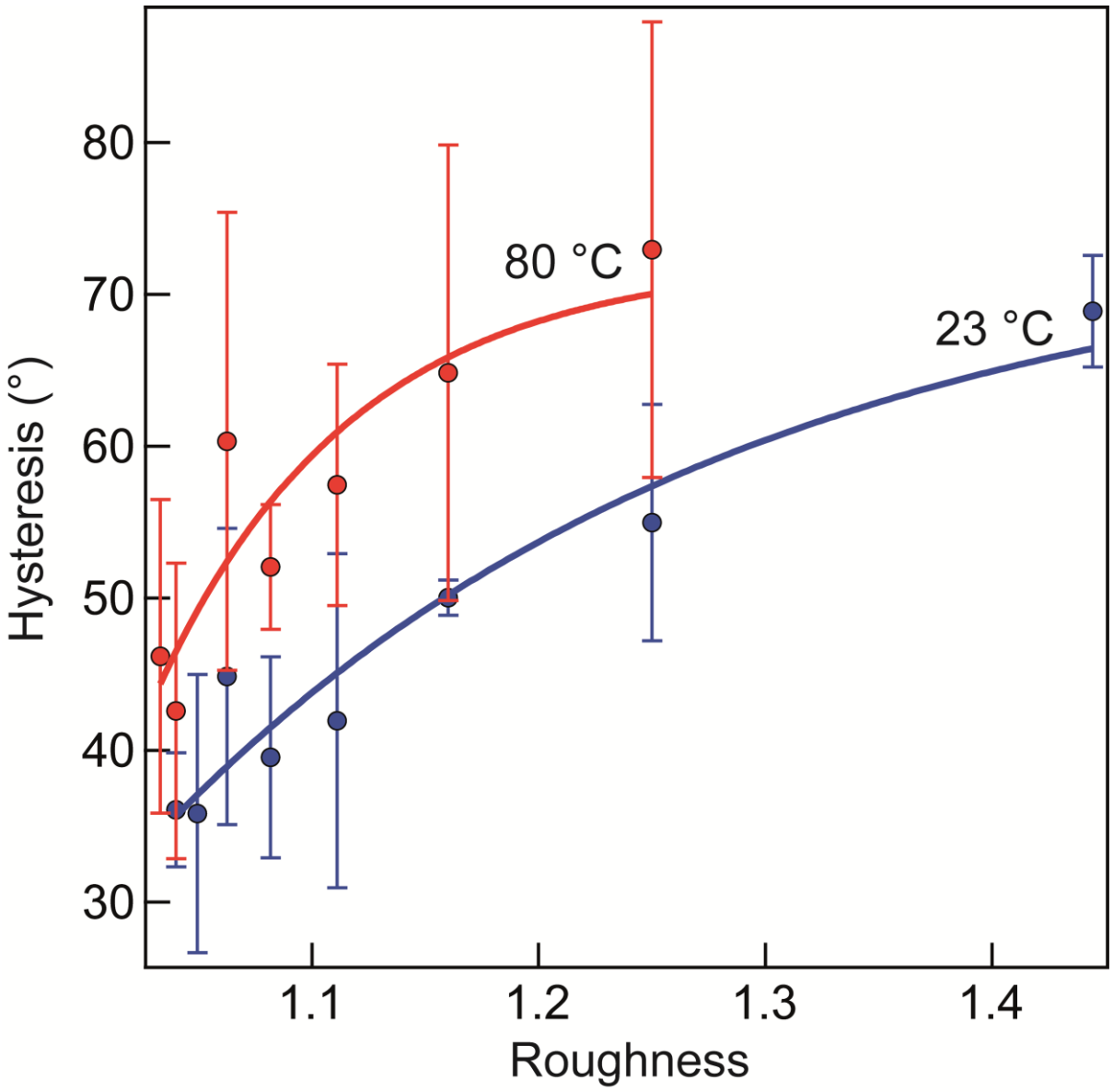

Figure 9: Contact angle hysteresis as a function of temperature for experiments performed at room temperature (23 degrees Celsius) and at 80 degrees Celsius.

Biographical details

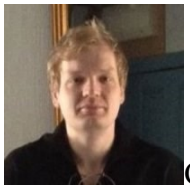 Coinneach Mackenzie-Dover is a Research Associate at the University of Edinburgh (Institute for Integrated Micro and Nano Systems). He has a PhD in Condensed Matter Physics subsequent to undergraduate studies at the University of Edinburgh. He is currently undertaking work examining the relationship between surface structure and wettability.

 Gail Duursma is a Lecturer in Chemical Engineering at the University of Edinburgh. She obtained her D.Phil. from the University of Oxford and after post-doctoral study at the University of Oxford, she joined the University of Edinburgh. She is a Member of the IChemE.

 John Christy is a Senior Lecturer at the University of Edinburgh. He holds an MEng degree in Chemical Engineering from the University of Cambridge. His PhD was completed at the University of Edinburgh, investigating the correlation between milk clot deposition and flow characteristics, with a view to gaining greater insight into thrombosis in blood flows.

 Jonathan G. Terry is a Chancellor's Fellow and Lecturer in the School of Engineering at the University of Edinburgh. He has worked at the University for over fifteen years primarily researching the development of more-than-Moore technologies, the integration of novel fabrication processes and materials with foundry CMOS to create smart sensors and microsystems. To date, he has worked on the development of sensing systems for physical, biological, chemical, medical and astronomical applications. His work has received a number of awards, including the IEEE ICMTS Best Paper 2004, IET Nanobiotechnology Premium Award 2008 and IJMS Best Paper 2013, and he has over 80 publications..

 Khellil Sefiane has MSc and PhD degrees in Chemical Engineering. He presently holds the Chair of Thermophysical Engineering at the University of Edinburgh. He is also ExxonMobil Fellow at the University of Edinburgh.In 2015 he was appointed Honorary Professor at Kyushu University.